

Coupling Heat Transfer and Fluid Flow Solvers for High Area Ratio Rocket Nozzle

Haifeng Hu⁺, Futing Bao and Qiang Cai

National Key Laboratory of Combustion, Flow and Thermo-Structure
Northwestern Polytechnical University
Xi'an, 710072, China

Abstract. Turbulent flow separation coupling heat transfer with the solid case in the high area ratio rocket nozzle is simulated with the CFD method and the results are investigated experimentally. The finite volume method, the 2nd order upwind scheme, SST k- ω turbulence model and enhanced wall function are employed to solve the N-S equation and thermal conduction equation. To predict the fluid field and wall temperature distribution, numerical models have been developed considering both solid and fluid regions. Solid and fluid regions work together, each one providing a boundary condition for the other, and the solution to the coupled problem has been attained. In the end, flow in a high area ratio rocket nozzle is simulated, separation is indicated, and in the separation zone the temperature gradient is high. The location of the separation point predicted agreed well with the experimental data, which proved the accuracy of the method of numerical simulation.

Keywords: High area ratio rocket nozzle, Fluid-thermal coupled analysis, Numerical simulation, Gas separation, Ground test

1. Main text

Nozzle design constitutes an important phase of rocket development. The performance of a rocket depends heavily on its nozzle's effectiveness in converting thermal energy to kinetic energy. To increase the vacuum performance of classical convergent-divergent rocket nozzles, it is desirable to achieve high expansion rate. Modern rocket nozzles are designed to operate over a wide range of altitudes and are typically with large area ratios to ensure high efficiencies at high altitudes. A nozzle's design altitude is where its exit pressure is equal to the ambient pressure. Above that altitude, the nozzle flow is 'underexpanded' and below it, 'overexpanded'. In both conditions the nozzle produces thrust less than the possible maximum value. Usually the nozzle design altitude is well above sea level, leaving the nozzle flow in an overexpanded state for its startup as well as ground testing. Overexpansion in a rocket nozzle presents the critical, and sometimes design driving, problem of flow separation induced side loads. The structure of the liquid-rocket-engine nozzle flow-field generated by the flow separation that may occur because of a strong overexpansion has attracted many experimental and numerical studies [1-15]. The reason why so many studies have been carried out on this subject is that the evolution of flow separation structure during nozzle startup seems to be the main factor responsible of the different side-load levels that take place in nozzles with different shapes.

In the present study, a new numerical method is adopted in the simulation of the separation flow in the rocket nozzle with high area ratio, carried out in a validated numerical Reynolds-Averaged-Navier-Stokes code, with turbulence computed according to two-equation SST model. In the end, an experiment is conducted to validate the results.

⁺ Corresponding author. Tel.: + (13891892342); fax: + (029-88493406).
E-mail address: (huhaifeng_rocket@126.com).

The paper is organized as follows: in next section, the governing equations of the flow and heat transfer of the solid case of the nozzle are briefly described. Then, results are presented and discussed in comparison with the experiment data, leading to the conclusions at the end of the paper.

2. Numerical Approach

The analysis of the nozzle flow field is performed by a 2D axisymmetric time-accurate perfect gas Reynolds-averaged Navier-Stokes solver. The finite volume method, the 2nd second upwind scheme, SST $k-\omega$ turbulence model and enhanced wall function are employed to solve the N-S equation and heat conduction equation. To simulate the fluid field and wall temperature distribution, numerical models have been developed considering both solid and fluid regions. Solid and fluid regions work together, each one providing a boundary condition for the other, and the solution to the coupled problem has been obtained.

2.1. Governing equations

The two dimensional, unsteady, compressible, time-averaged Navier–Stokes equations and conservation equations for mass, energy, turbulent kinetic energy, and species transfer are written as follows in a general form:

$$\frac{\partial(\rho\phi)}{\partial t} + \text{div}(\rho\bar{U}\phi) = \text{div}(\Gamma_\phi \text{grad}\phi) + S_\phi \quad (1)$$

Where ϕ is any dependent field variable, \bar{U} stands for the gas velocity vector, ρ is the gas density and Γ represents the exchange coefficient such as the diffusion coefficient. S_ϕ is the source term stemming from the turbulent flow field. SST $k-\omega$ turbulence model and enhanced wall function are utilized to solve the N-S equation to acquire the flow parameters.

Energy equation of the flow field is in the following form:

$$\frac{\partial}{\partial t}(\rho E) + \frac{\partial}{\partial x_i}(u_i(\rho E + p)) = \frac{\partial}{\partial x_i} \left(k_{\text{eff}} \frac{\partial T}{\partial x_i} - \sum_j H_j M_j + u_j (\tau_{ij})_{\text{eff}} \right) + S_h \quad (2)$$

Where E stands for the energy, u_i the velocity, p the pressure, k_{eff} the effective conductivity, H_j the sensible enthalpy and M_j the diffusion flux of species j . The first three terms on the right-hand side of Equation (2) represent energy transfer due to conduction, species diffusion, and viscous dissipation, respectively. S_h is the sources term. T means the temperature.

The heat conduction equation in solid case can be written as:

$$\frac{\partial}{\partial t}(\rho H) + \frac{\partial}{\partial x_i}(\rho u_i H) = \frac{\partial}{\partial x_i} \left(k \frac{\partial T}{\partial x_i} \right) + S_h \quad (3)$$

H is the sensible enthalpy and $H = \int_{T_{\text{ref}}}^T c_p dT$. T_{ref} means the reference temperature, and c_p stands for the specific heat.

Coupled thermal boundary analysis:

(a) the temperature must continue at the coupled boundary of the hot gas-solid interface:

$$T_w |_{\text{I}} = T_w |_{\text{II}} \quad (4)$$

(b) the third thermal boundary condition at the hot gas-solid interface:

$$-\lambda \left(\frac{\partial T}{\partial n} \right)_w |_{\text{I}} = h(T_w - T_f) |_{\text{II}} \quad (5)$$

λ is the conductivity and h means the convective heat transfer coefficient. Subscript w stands for the wall and f the hot gas.

2.2. Numerical Method

Axisymmetric two-dimensional simulations under experimental conditions are conducted to examine details of the flow field inside the nozzle such as the location of the separation point and the separation

patterns. The numerical method is based on a finite difference method to solve the Reynolds-averaged Navier-Stokes (RANS) equations. The accuracy in time and space are both second orders. The viscous fluxes are evaluated with second-order central-difference scheme. Diffusive terms are handled by central differencing, using Sutherland's law for transport properties. Turbulence is treated according to a Reynolds-Averaged Navier-Stokes equations approach. The turbulent viscosity is modeled according to the two-equation model SST. The time integration is done in a backward three-point difference scheme with sub-iterations in each time steps implemented with the LU-SGS method [16].

This paper takes two steps to get the simulation results of the given computation model. First, the steady method is employed to get the steady flow field of the nozzle at different combustion pressure, then the results are treated as the initial flow condition of the transient analysis coupling heat transfer with the solid case of the nozzle.

3. Results And Discussions

Figure 1 illustrates the computational and the experiment model of large area ratio nozzle profile. The nozzle is designed with a thrust-optimized contour, and its expanded area ratio is 55.2. Detail parameters of the nozzle are also shown. The combustion pressure is 6MPa, double base propellant is chosen for the grain, total temperature of the hot gas is about 2300K, and Sutherland's law for transport properties is applied. The rocket motor works for 2.5 seconds. The outlet boundary is set as pressure outlet, its value equals to the ambient pressure. During the steady state analysis, the solid zone are not taken into consideration. When it comes to flow-thermal coupled analysis, steady state results are treated as the initial flow condition.

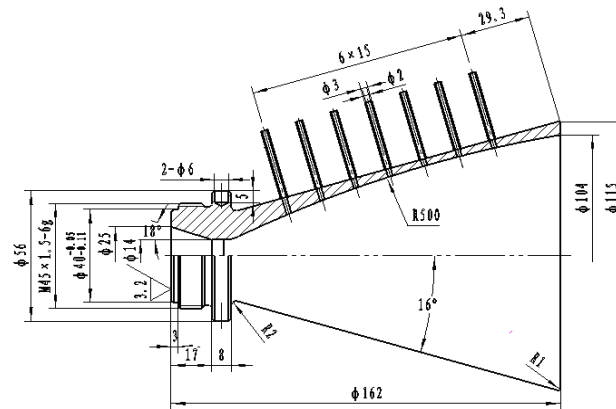


Fig. 1 simulation model scheme of the nozzle

3.1. Steady State Analysis

If the ambient pressure is greater than that of the nozzle flow, it is possible for the ambient pressure to force its way upstream along the wall, causing the flow to separate from the nozzle wall and a recirculation zone to appear. If the nozzle flow separates, pressure difference between the inner and outer nozzle surfaces is created.

Figure 2 shows the velocity magnitude contour of the nozzle at different combustion pressure ranging from 2MPa to 7MPa with an increment of 1MPa. It can be found that the separation points vary with different combustion pressure. There is only one shock pattern - free shock separation (FSS) when the combustion pressure changes from 2MPa to 7MPa. FSS means that the boundary layer separates from the nozzle wall and never reattaches back. The computations are carried out at seven different Nozzle Pressure Ratio (NPR): 19.74, 29.61, 39.48, 49.35, 59.22, and 69.08. From Figure 2, it can be observed that for the given nozzle contour, flow separation always occur under these working conditions, and the separation point moves towards the exit as the combustion pressure increasing, but the shock pattern remains unchanged.

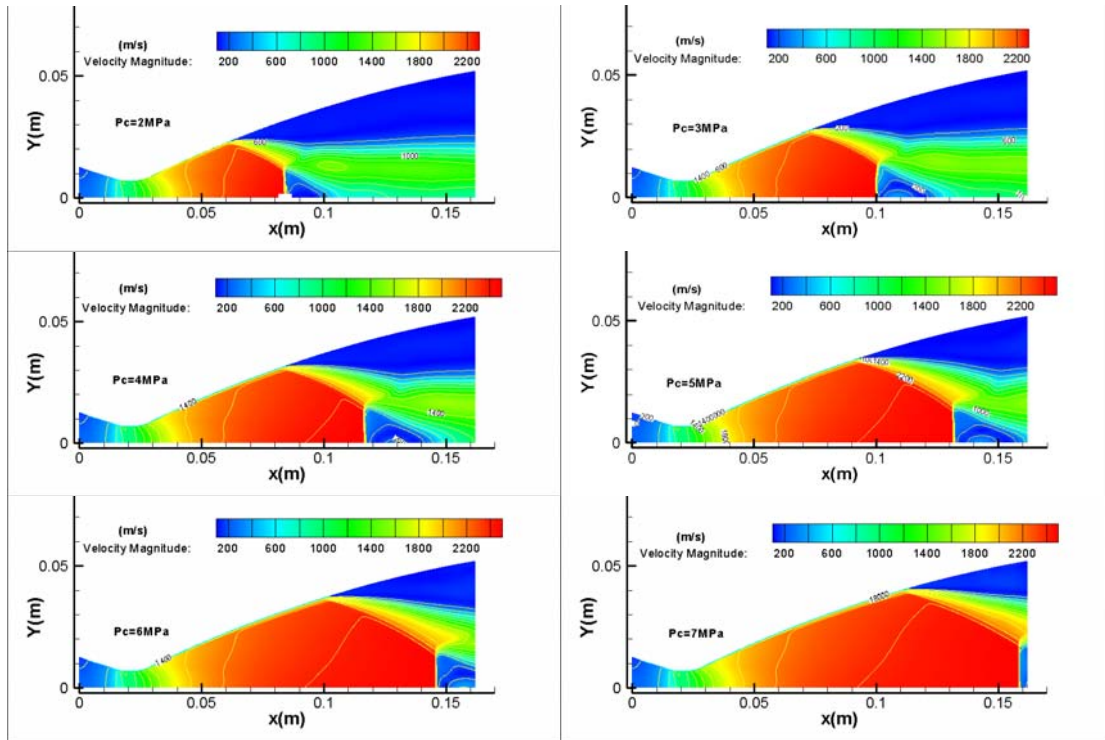


Fig. 2 velocity magnitude contour of the nozzle at different combustion pressure which from 2MPa to 7MPa

Pressure distribution along the nozzle is shown in Figure 3. At separation points, pressure rises. Flow separation is a result of adaptation to the ambient pressure. Because the area ratio is large, flow in the nozzle is over expanded, and adaptation to ambient pressure induces the flow separation. From Figure 2 an oblique shock wave can be identified, through which the flow parameters change sharply. As the ambient pressure is 1 atm, pressure after the separation point all shifts to 1 atm.

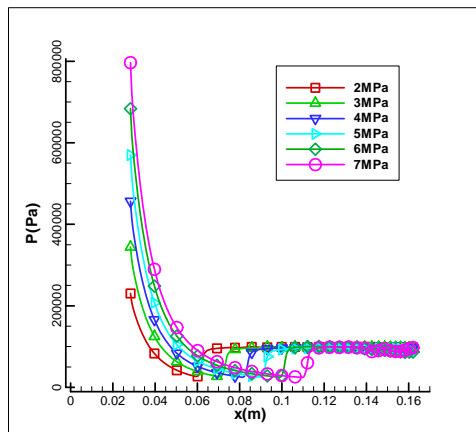


Fig. 3 pressure distribution curve along the nozzle wall

Heat transfers between hot gas and the nozzle wall by way of convection and radiation. Compared with radiation, convection plays a more important part. Incorporating the Bartz equation [17], the convective heat coefficient of the nozzle can be obtained.

Figure 5 shows the convective heat transfer coefficient of the diverging section of the nozzle. It is quite obvious that the convective heat transfer coefficient rises after the separation point. The flow separation occurs at the location of the oblique shockwave, through which aerodynamic parameters alter drastically, bringing changes to the coefficient, which in turn imposes a rigorous thermal condition on the material of the nozzle structure.

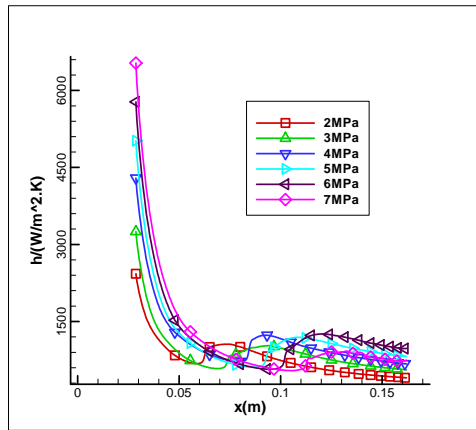


Fig. 4 the convection heat transfer coefficient of the diverging section of the nozzle

3.2. Transient Analysis

After the steady state analysis, transient analysis is done to find out the thermal condition when flow separation occurs. The steady state results are treated as the initial flow condition. The rocket works for 2.5 seconds.

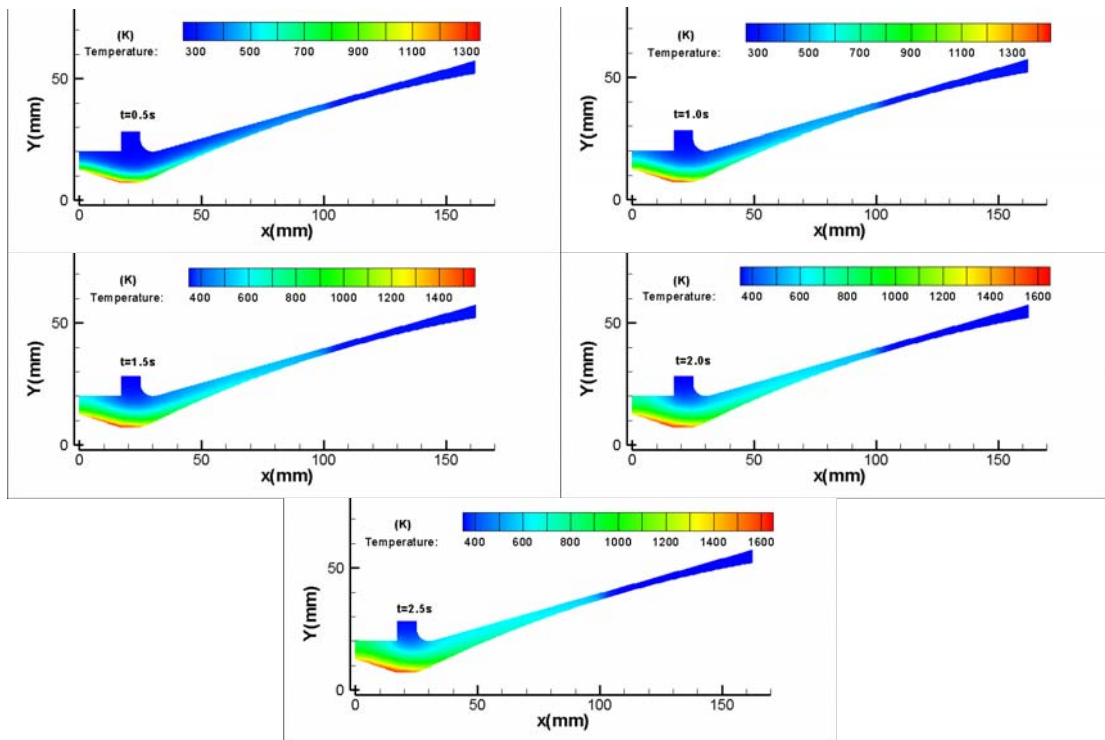


Fig. 5 the temperature contour of the nozzle case at different time which from 0.5s to 2.5s

Figure 5 illustrates the temperature contours of the nozzle at different work time. It can be found that the highest temperature is located near the nozzle throat.

Figure 6 shows the interior temperature distribution of the nozzle wall. The highest temperature is situated near the throat because the gas temperature in the converging section is high and the flow parameters through the throat shift dramatically, the convective heat transfer is very strong. Dramatic temperature change can also be found at the separation point. The steep gradient near the separation point exerts harsh thermal load on the nozzle, which means that when flow separation occurs, thermal load near the separation point is as harmful as side load, and cannot be ignored.

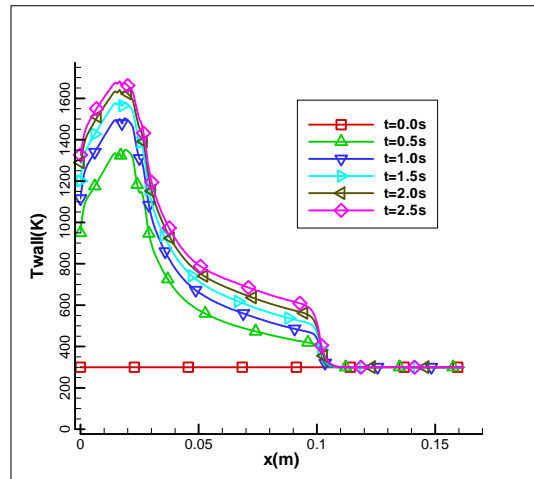


Fig. 6 the interior temperature distribution of the nozzle wall along the axis at different time

3.3. Experiment Compared

In order to validate the numerical results, a set of experiment system was designed and ground tests were performed. The drawing of the test rocket nozzle and the distribution of the sensors are shown in Figure 1.

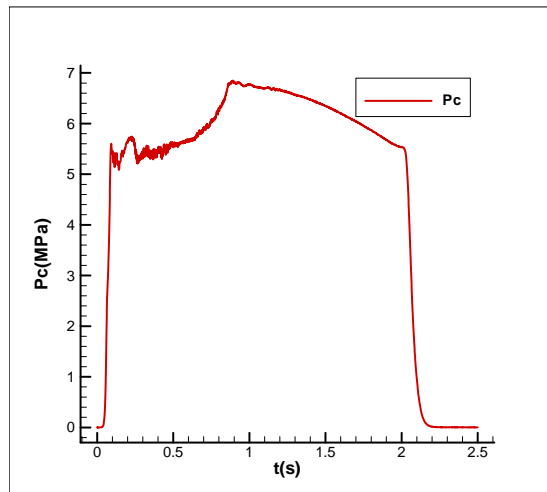


Fig. 7 test pressure-time history of the combustor

The sensor was mounted on the combustor wall and 7 on the nozzle wall in order their sensing elements be in flush with the inner nozzle surface. Data from the sensors were simultaneously acquired by a Dewetron Data Acquisition System. Figure 7 illustrates the combustor pressure-time history.

Figure 8 shows the comparison between simulated pressure distributions along the nozzle wall and the experiment data. The two reached quite good agreement and the effectiveness of the method is thus validated.

4. Conclusions

Numerical simulation of the flow separation in high area ratio rocket nozzle has been carried out with the CFD method. The flow field and thermal field of the nozzle were simulated for the given nozzle contour. The results indicated that with NPR ranging from 19.74 to 69.08, the shock pattern remains FSS, and near the flow separation point, the temperature gradient is steep, so the thermal load cannot be ignored when analyses are implemented.

At last, experiments were conducted to validate the computational results, and the shockwave was captured. The pressure distribution predicted agreed well with the experiment data, and the effectiveness of the method therefore got verified.

5. References

- [1] Frey, M. and Hagemann, G., "Status of Flow Separation Prediction in Rocket Nozzles," AIAA Paper 98-3619, July 1998, 34th AIAA/ASME/SAE/ASEE Joint Propulsion Conference.
- [2] Onofri, M. and Nasuti, F., "The Physical Origin of Side Loads in Rocket Nozzles," AIAA Paper 99-2587, July 1999, 35th AIAA/ASME/SAE/ASEE Joint Propulsion Conference.
- [3] Chen, C. L., Chakravarthy, S. R., and Hung, C. M., "Numerical Investigation of Separated Nozzle Flows," AIAA Journal, Vol. 32, No. 9, 1994, pp. 1836-1843. doi: 10.2514/3.12181
- [4] Frey, M. and Hagemann, G., "Restricted Shock Separation in Rocket Nozzles," Journal of Propulsion and Power, Vol. 16, No. 3, 2000, pp. 478-484. doi: 10.2514/2.5593
- [5] Frey M., Stark R., Ciezki H., Quessard F., and Kwan W., "Subscale Nozzle Testing at the P6.2 Test Stand", AIAA Paper 2000-3777, 2000.
- [6] Gross A., Haidn O., Stark R., Zeiss W., Weber C., and Weiland C., "Experimental and Numerical Investigation of Heat Loads in Separated Nozzle Flow", AIAA Paper 2001-3682, 2001.
- [7] Stark R., Kwan W., Quessard F., Hagemann G., and Terhardt M., "Rocket Nozzle Cold-Gas Test Campaigns for Plume Investigations", 4th European Symposium on Aerothermodynamics for Space Vehicles, Capua, 2001.
- [8] Kwan W., and Stark R., "Flow Separation Phenomena in Subscale Rocket Nozzles", AIAA Paper 2002-4229, 2002.
- [9] Deck, S. and Guillen, P., "Numerical Simulation of Side Loads in an Ideal Truncated Nozzle," Journal of Propulsion and Power, Vol. 18, No. 2, Mar-Apr 2002, pp. 261-269. doi: 10.2514/2.5965
- [10] Watanabe, Y., Sakazume, N., and Tsuboi, M., "LE-7A Engine Nozzle Problems during the Transient Operations," AIAA Paper, AIAA 2002-3841, 2002.
- [11] Yonezawa, K., Yamashita, Y., Tsujimoto, Y., Watanabe, Y., and Yokota, K., "A Numerical Study of Flow Structure in Over-Expanded Rocket Nozzles," Proceedings of Asian Joint Conference on Propulsion and Power, edited by JSASS, 2004, pp. 212-219.
- [12] Reijasse, P., "Aerodynamics of overexpanded propulsive nozzles : free separation and side loads in stabilized regime," Ph.D. dissertation, University of Pierre-et-Marie-Curie, Paris 6-Jussieu, Paris, France, 2005.
- [13] Kurt B. Smalley, Andrew M. Brown, Ph.D., Joseph Ruf. "Flow Separation Side Loads Excitation of Rocket Nozzle FEM". 48th AIAA/ASME/ASCE/AHS/ASC Structures, Structural Dynamics, and Materials Con 23-26 April 2007, Honolulu, Hawaii. AIAA 2007-2242
- [14] Francesco Nasuti, Marcello Onofri, and Emanuele Martelli. "Numerical Analysis of Flow Separation Structures in Rocket Nozzles". 43rd AIAA/ASME/SAE/ASEE Joint Propulsion Conference & Exhibit 8-11 July 2007, Cincinnati, OH, AIAA 2007-5473
- [15] Gerald Hagemann, Manuel Frey. "Shock pattern in the plume of rocket nozzles: needs for design consideration". Shock Waves, Vol. 4, No. 2, July-August 2008, pp. 387-395, doi: 10.1007/s00193-008-0129-y
- [16] ANSYS INC, Fluent User Manual 2007
- [17] Bartz, D.R., "A simple Equation for Rapid Estimation of Rocket Nozzle Convective Heat Transfer Coefficients", ARS Journal, Jan 1957, p 49-53.